ISSN 2229-5518

Study of Magnatohydrodynamics on a Boundary Layer Flow over Nonlinear Stretching Sheet with Injection/Suction and Thermal Radiation

Pudhari Srilatha[1] and M N Raja Shekar[2]
[1]Research Scholar, Department of Mathematics, Rayalaseema University, Kurnool, AP, India.
[2]Department of Mathematics, JNTUH College of Engineering, Nachupally, Jagitial, TS, India.

Abstract— the paper deals with the study of magnatohydrodynamics (MHD) on a boundary layer flow over a nonlinear stretching sheet with suction or an injection in the thermal radiation. The partial differential equations were reduced to higher order ordinary differential equations using of Keller- Box method in the present studies. The velocity, temperature and nanoparticle fluid concentration, local skin friction coefficient, local Nusselt number and local Sherwood number are affected by the governing parameters. It is found that the dimensionless velocity decreases and temperature, nanoparticle fluid concentration are increased with increasing on magnetic parameter.
Index Terms— Magnatohydrodynamics, Nanofluid, Thermal radiation, Stretching sheet, Boundary layer, Keller – Box, Stretching sheet.

——————————   ◆   ——————————

1 INTRODUCTION

Boundary layer behaviour with heat and mass transfer over a nonlinear stretching sheet in presence of the thermal radiation is very important for various engineering and industrial applications. Grubka *et.al*[4] studied the effect of heat transfer characteristics of a boundary layer flow of fluids over a linear continuous stretching surface. Chen *et.al.*[5] studied the heat transfer effect of boundary layer flow over a linear stretching sheet which was subjected to suction/ blowing in the present of the sheet with prescribed wall temperature and heat flux. Kumaran *et.al* [6] examined the transition effect of boundary flow due to a presence and an absence of magnetic field over a various flow past a stretching sheet and analyzed the task numerically by implicit finite difference technique. Basker *et.al*[7] investigated the steady laminar flow over a stretching sheet with a convective boundary condition by the considering of the effect of partial slip. Ali *et.al*[8] studied the steady laminar magnetohydrodynamics (MHD) mixed convection stagnation point flow of an incompressible viscous fluid over a vertical stretching sheet. Zaimi *et.al.*[9] examined the flow, heat along with the mass behaviour transfer over a nonlinear stretching/shrinking sheet in a nanofluid. Few researchers studied on the boundary layer flow over linear stretching sheet[10-14] and nonlinear stretching sheet[15-17].

Nano-fluids are mainly used for coolant in heat transfer apparatus like radiations, heat exchangers and electronic cool units. Ibrahim and shankar[18] have numerically examined the boundary – layer flow and heat transfer of nano-fluid over a vertical plate with convective surface boundary condition, the study shows that the local Nusselt number and local Sherwood number increase in convective parameter and Lewis number. The effects of thermal radiation and viscous dissipation on MHD stagnation point flow and heat transfer over a nano-fluid is studied by Yirga and Shankar[19]. The boundary layer flow and heat transfer over a non-isothermal stretching sheet in nano-fluid have been studied numerically with the effect of magnetic field and thermal radiation[20].

The main objective of the present paper is to solve the problem of magnetohydrodynamics(MHD) studies on boundary layer flow over nonlinear stretching sheet with injection/suction and thermal radiation of a nano-fluid by adopting the well known Keller- Box method.

2 FROMULATION OF THE PROBLEM

Consider a two dimensional steady laminar boundary layer flow over a permeable nonlinear stretching sheet in the presence of MHD in an incompressible viscous fluid. Presume sheet direction is horizontal with the x-axis and y-axis is the direction normal to the stretching sheet. Presented flow is restricted to $y > 0$ and is due to the simultaneous effect of two equal and opposite forces along the direction of the x-axis and maintained the origin is fixed. The sheet coincides with the plate $y = 0$ and its velocity is assumed as $u_w = ax^n$ here 'a' and 'n' are positive constant values (Figure 1).

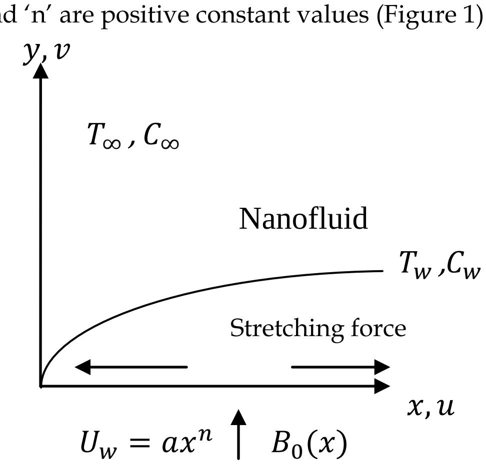

Fig.1. Flow organization with coordinate system.

ISSN 2229-5518

The boundary layer equations under the Boussinesq approximations and for steady state flow conditions are given by:

$$\frac{\partial u}{\partial x}+\frac{\partial u}{\partial y}=0 \quad \text{... (1)}$$

$$u\frac{\partial u}{\partial x}+v\frac{\partial u}{\partial y}=\nu\frac{\partial^2 u}{\partial y^2}-\frac{\sigma}{\rho}B_0^2(x)u \quad \text{... (2)}$$

$$u\frac{\partial T}{\partial x}+v\frac{\partial T}{\partial y}=\alpha\frac{\partial^2 u}{\partial y^2}-\frac{\partial q_r}{\partial y} \quad \text{... (3)}$$

$$u\frac{\partial C}{\partial x}+v\frac{\partial C}{\partial y}=D\frac{\partial^2 C}{\partial y^2} \quad \text{... (4)}$$

with boundary conditions:

$$\begin{cases} u=U_w(x)=ax^n, v=v_w(x), T=T_w, C=C_w \ \ at \ \ y\to 0 \\ u\to 0, \ T\to T_\infty, C\to C_\infty \quad as \quad y\to\infty \end{cases}$$

The following shifts are used to transform the governing partial differential equations in to a scheme of ordinary differential equations.

$$\eta=y\left(\frac{a(n+1)}{2\nu}\right)^{\frac{1}{2}}x^{\frac{1}{2}}, \ f'=F, \ u=\frac{\partial\varphi}{\partial y}, \ v=-\frac{\partial\varphi}{\partial x}, u=ax^n f'$$

$$\varphi(x,y)=\left(\frac{2a\nu}{n+1}x^{n+1}\right)^{\frac{1}{2}}f\ \ \eta\ , G(\eta)=\frac{T-T_\infty}{T_w-T_\infty}, S_c=\frac{\nu}{D}, P_r=\frac{\nu}{\alpha},$$

$$H(\eta)=\frac{C-C_\infty}{C_w-C_\infty}, v=-\sqrt{\frac{a\nu(n+1)}{2}}x^{\frac{n-1}{2}}\left(f+\eta\left(\frac{n-1}{n+1}\right)f'\right),$$

The similarity variable and dimensionless stream function satisfy the continuity equation. By invoking the Rossel and approximation given by Cortell[21] the radiative heat flux can be written as:

$$q_r=-\frac{4\sigma^*}{3k^*}\frac{\partial T^4}{\partial y} \quad \text{... (5)}$$

Here σ^* and k^* are the Stefan-Boltzman constant and the mean absorption coefficient, respectively. The temperature differences within the flow region are assumed to be the term T^4 which can be expressed as a linear function of temperature. Using the Taylor series expansion to T^4 about T_∞ and neglecting higher order terms, we have

$$T^4\cong 4T_\infty^4 T-3T_\infty^4 \quad \text{... (6)}$$

Using the above said transformations and in view equation (5) and (6), equation (3) becomes

$$u\frac{\partial T}{\partial x}+v\frac{\partial T}{\partial y}=\left(\alpha+\frac{16}{3}\frac{\sigma^* T_\infty^3}{\rho c_p k^*}\right)\frac{\partial^2 T}{\partial y^2} \quad \text{... (7)}$$

Considering $N_R=\frac{kk^*}{4\sigma^* T_\infty^3}$ radiation parameter, the equation (7) becomes to

$$u\frac{\partial T}{\partial x}+v\frac{\partial T}{\partial y}=\left(\frac{\alpha}{k_0}\right)\frac{\partial^2 T}{\partial y^2} \quad \text{... (8)}$$

Here $k_0=\frac{3N_R}{3N_R+4}$ with the similarity variable η , the equations (2), (8) and (4) reduces to the following ordinary differential equations, respectively

$$f'''+ff''-\frac{2n}{n+1}\ f'^{\,2}-Mf'=0 \quad \text{... (9)}$$

$$G''+k_0P_r fG'=0 \quad \text{... (10)}$$

$$H''+ScfH'=0 \quad \text{... (11)}$$

with boundary conditions:

$$f(0)=s, f'(0)=1, G(0)=1, H(0)=1 \ \ at \ \ \eta=0 \quad \text{... (12)}$$

$$f'\to 0, G\to 0, H\to 0 \quad as \quad \eta\to\infty \quad \text{... (13)}$$

Here $s=\frac{-v_w(x)}{\sqrt{a\nu\frac{(n+1)}{2}x^{n-1}}}$ is the suction/injection parameter and $s<0, s>0$ & $s=0$ belongs to injection, suction and impermeability case respectively. The physical quantities of importance from the engineering point of observations are the skin friction coefficient (C_{fx}), local Nusselt number (Nu_x) and local Sherwood number (Sh_x) which are defined as

$$C_{fx}=\frac{2\tau_w}{\rho u_w^2} \quad \text{... (14)}$$

$$Nu_x=\frac{xq_w}{k\ \ T_w-T_\infty} \quad \text{... (15)}$$

$$Sh_x=\frac{xq_m}{D\ \ C_w-C_\infty} \quad \text{... (16)}$$

Here the wall heat flux q_w and the mass flux q_m are given as:

$$\tau_w=\mu\left.\frac{\partial x}{\partial y}\right|_{y=0}, \ q_w=-k\left.\frac{\partial T}{\partial y}\right|_{y=0}, q_m=-D\left.\frac{\partial C}{\partial y}\right|_{y=0}$$

Using of similarity variable, the equation (14), (15) and (16) becomes:

$$f''(0)=C_f\left(\sqrt{\mathrm{Re}_x/2(n+1)}\right) \quad \text{... (17)}$$

$$-G'(0)=Nu_x\Big/\sqrt{\mathrm{Re}_x\left(\frac{n+1}{2}\right)} \quad \text{... (18)}$$

$$-H'(0)=Sh_x\Big/\sqrt{\mathrm{Re}_x\left(\frac{n+1}{2}\right)} \quad \text{... (19)}$$

3 NUMERICAL PROCEDURE

The partial differential equations were reduced to higher order ordinary differential equations using of suitable similarity transformations and further these are solved numerically using Keller-Box method in the present studies. The nonlinear ordinary differential equations of (9), (10) and (11) with boundary conditions (12) and (13) are solved. The parameters for the present study are magnetic parameter (M), Prandtlnumber (Pr), Schmidt number (Sc), suction/injection parameter(s), radiation parameter (Nr), and the nonlinear stretching sheet parameter (n). The numerical values are evaluated and tabulated in tables I, II and graphs are presented in figures 2 to 14 for various values of physical parameters.

ISSN 2229-5518

4 RESULTS AND DISCUSSION

To find the numerical explanation for the specified problem, a parametric study is carried out to demonstration the effects of its governing parameters. Figure 2 and 3 illustrates the effect of magnetic and nonlinear stretching parameters on the dimensionless velocity. It is evidently observed that the velocity profile of nanoparticle fluid is insignificantly reduced with increasing values of *M* and *n.* The velocity is reduced strongly as the results of increased magnetic field, and is due to the act transverse to the direction of the functional magnetic field, and is well known as Lorentz force, which will decelerate the boundary layer flow and the thickness of the momentum boundary layer. Hence this will encourage an increase of the velocity gradient at its surface as clearly expressed in figures. An effect of magnetic and nonlinear stretching sheet parameters on the temperature profile is presented in figure 4 and figure 5. It is evidently observed that the temperature of the nanoparticle fluid is increasing as increase in the magnetic field as well as nonlinear stretching sheet parameters. From figure 4, the temperature profile is increased from injection to suction case as *M* is increase, whereas if then is increasing the temperature profile is increased from suction to injection.

Figure 6 and 7 exhibits the effects of magnetic and nonlinear stretching sheet parameters on the nanoparticle fluid concentration. It indicates that the nanoparticle fluid concentration is increasing as increase in the magnetic field and the nonlinear stretching sheet parameter. From these figure 6 and 7, the concentration profile is increased from suction to injection as M and n are increasing. The Lorentz force is a resistive force which will oppose the nanoparticle fluid motion, hence the heat is produced and as a result the thermal boundary layer thickness and nanoparticle fluid volume fraction boundary layer thickness turn into thicker from stronger magnetic field.

In figure 8, we observed that the increasing the radiation parameter *Nr* decrease the temperature of the fluid in the presence of a magnetic field. In the presence of magnetic field, the thermal boundary layer is also decreasing and is more injection than the suction. Impact of Prandtl number on the temperature profile is given figure 9, and indicates that increasing the Prandtl number as the decrease in the temperature and thermal boundary layer thickness is thick in injection than suction as in the presence of a magnetic field. A similar performance can be drawn to the effect of Schmidt number (Sc) on the species concentration in the magnetic field as is is indicated in the figure 10, i.e in the magnetic field, the variation is more in the suction than the injection. The figure 11 indicates the suction/injection parameter(s) increase during the velocity profile is decreasing and the other parameters are fixed.

Now, we focus on the variations of quantities of the physical interest from an engineering point of view. That, is local skin friction (C_{fx}), the local Nusselt number (Nu_x) and the local Sherwood number (Sh_x). From figure 12 indicates of that for the larger values of magnetic parameters M, the skin friction coefficient shows the increasing behaviour corresponds to the raise in the values of nonlinear stretching sheet parameter n. This means nanoparticle fluid motion on the wall of the sheet is accelerated when we strength the effect of parameters.

Figure 13 depicts the variation of the heat transfer rate with magnetic field and nonlinear stretching sheet parameter at different Prandtl number. It is experiment that the Nusselt numbers decrease with the increase in magnetic parameter and nonlinear stretching sheet parameter values. Figure 14 demonstrate the concentration variation with magnetic field and nonlinear stretching sheet for different values of Schmidt number. It is notice that the transformation of the dimensionless Sherwood number is found to be reduced slightly with the magnetic parameter M and nonlinear stretching sheet parameter n.

In the absence of magnetic parameter M the Skin friction coefficient, Nusselt number and Sherwood number are presented numerically in the Table I, whereas the Table II gives the values of Skin friction coefficient, Nusselt number and Sherwood number in the presence of variation of magnetic parameter and keeping the other parameter values fixed. It is clear from the Table II, the Nusselt number and Sherwood number are increasing function of *M* and the Skin friction coefficient can be observed decreased manner of increasing values of *M.*

5 CONCLUSIONS

MHD boundary layer and heat transfer of a nano fluid over a nonlinear stretching sheet in the presence of a thermal radiation wit suction/injection have been studied in the current paper. A similarity solution is presented which depend on Prandtl number, magnetic, nonlinearity of stretching sheet and thermal radiation, Schmidt number, and Suction/injection parameters. The effects of governing parameters on the flow, that is, on the velocity of the flow, concentration, skin friction coefficient and surface heat and mass transfer characteristics are discussed graphically and also numerically. The main observations of the present study are as follows:

- With the increasing of magnetic field, the velocity of the nanoparticle fluid decreases whereas the temperature and species concentration increases.
- Increase in nonlinear stretching sheet parameter reduces the velocity, enhances the temperature and species concentration.
- As increase in Prandtl number and thermal radiation there is a decrease in the temperature of the fluid.
- As Schmidt number increases the species concentration decreases.
- Increasing of nonlinear stretching sheet parameter, magnetic field results in diminish of skin friction coefficient.
- With the increase of magnetic and stretching sheet parameter there is an increase in the Nusselt number with the increase of Prandtl number.
- With the increase of magnetic and stretching parameter there is an increase in the Sherwood number with the increase of Schmidt number.

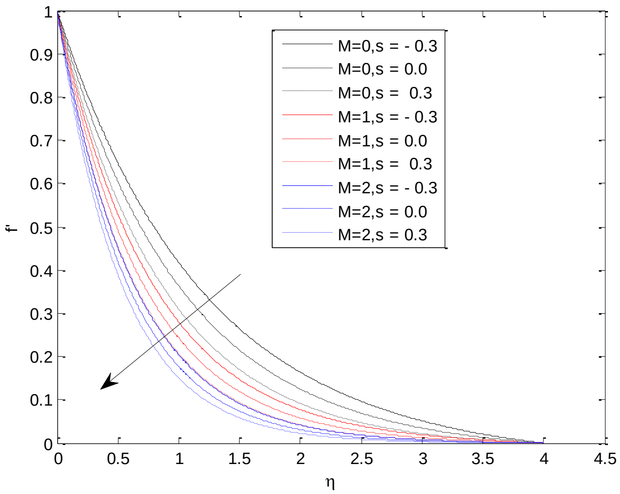

Fig .2. Velocity profile for various M values when Pr = 0.9, Nr=10, n= 1, Sc = 0.62

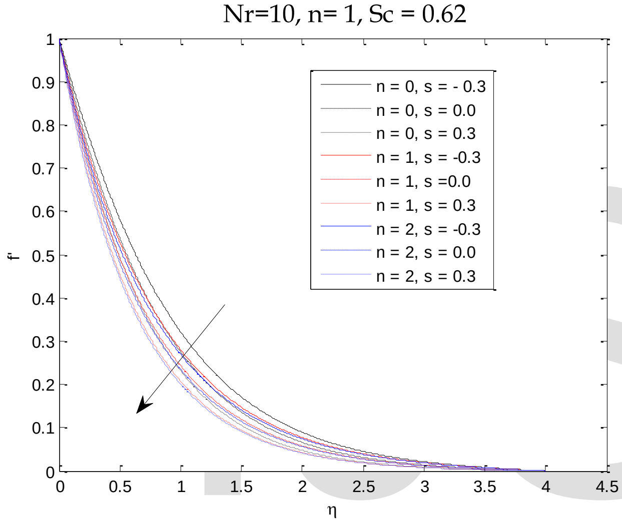

Fig .3. Velocity profile for various n values when. $Pr = 0.9, Nr = 10, M = 1, Sc = 0.62$.

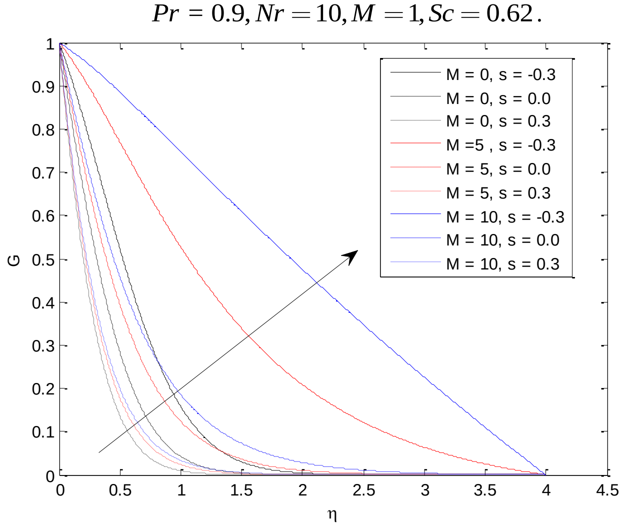

Fig .4. Temperature profile for various M values when $Pr = 7,\ Nr = 10, n = 1,\ Sc = 0.23$.

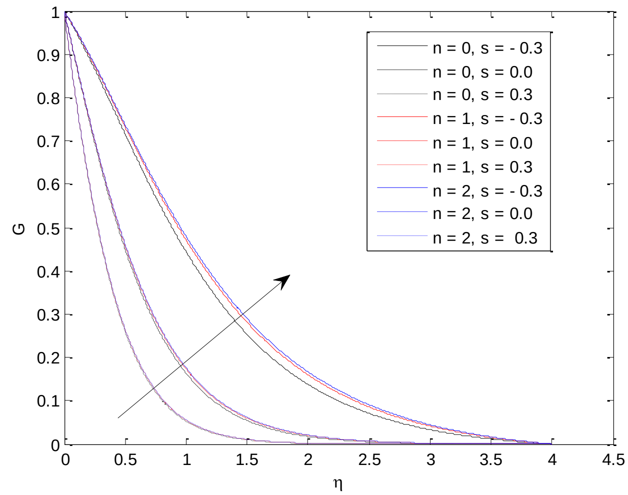

Fig .5. Temperature profile for various M values when $Pr = 5, Nr = 10, M = 3, Sc = 0.23$.

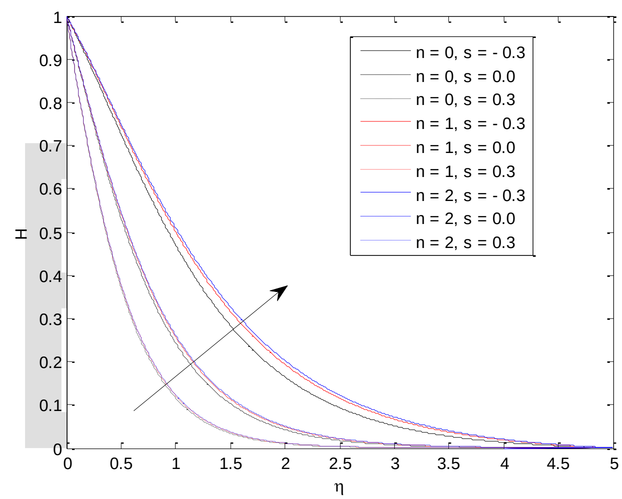

Fig .6. Concentration profile for various n values when $Pr = 0.5, Nr = 10, M = 2, Sc = 3$.

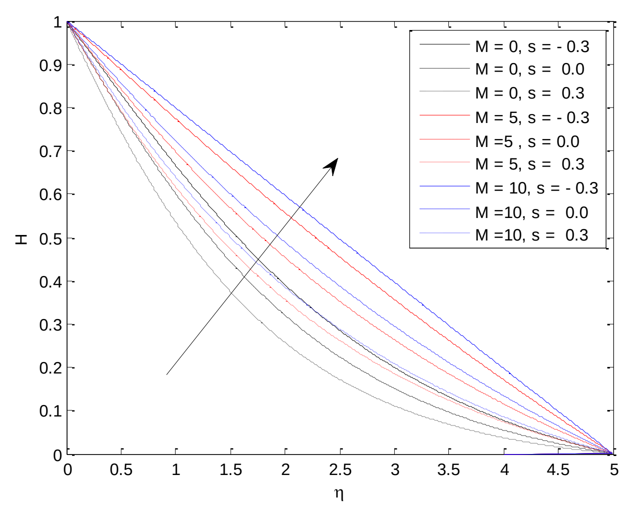

Fig.7. Concentration profile for various M values when $Pr = 0.7, Nr = 10, n = 2, Sc = 0.62$

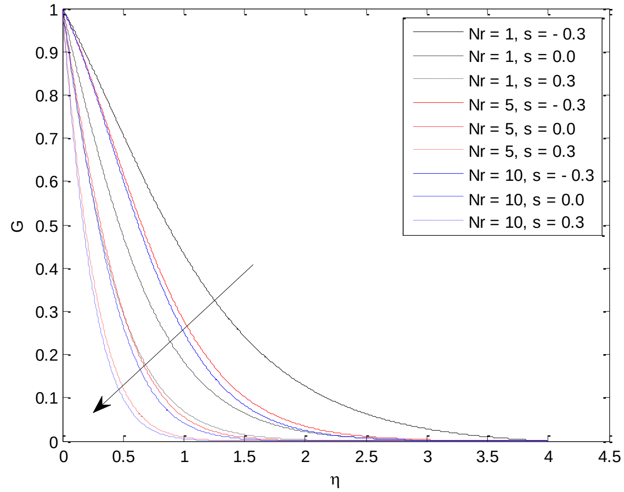

Fig .8. Temperature profile for various Nr values when $Pr = 9, n = 1, M = 2, Sc = 0.23$.

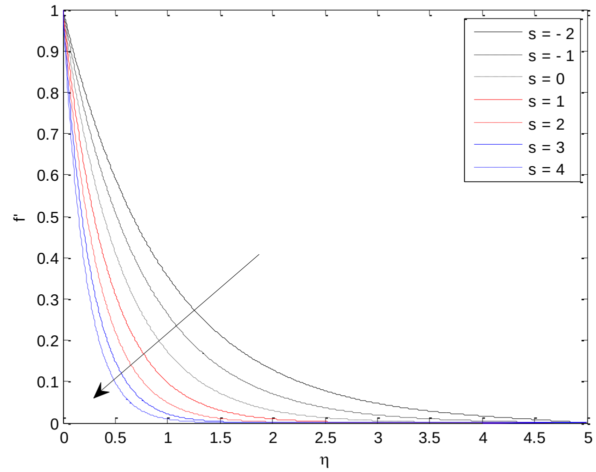

Fig .11. Velocity profile for various s values when $Pr = 0.5, Nr = 10, n = 2, M = 2, Sc = 0.23$

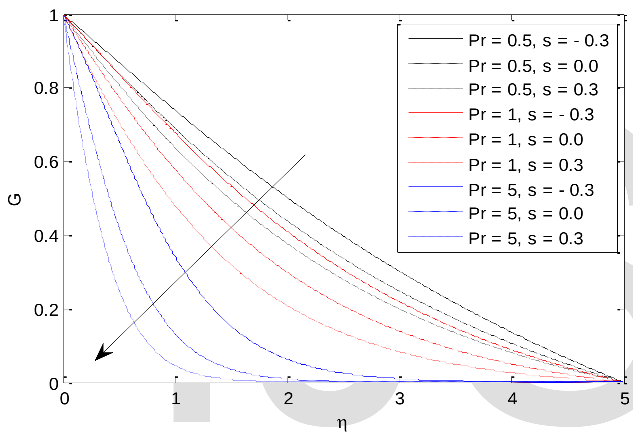

Fig .9. Temperature profile for various Pr values when $Nr = 9, n = 3, M = 1, Sc = 0.23$.

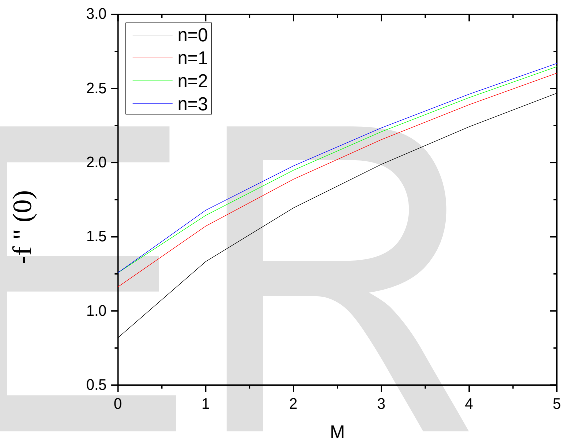

Fig. 12. Effect of M on skin friction coefficient when $Pr = 7, Sc = 0.62, \; Nr = 10, s = 0.3$

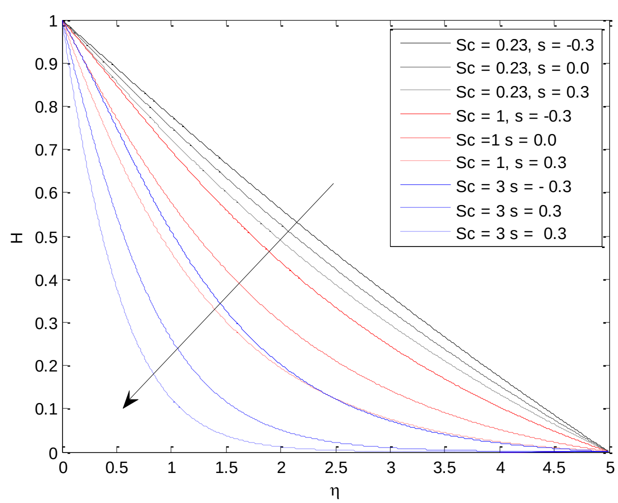

Fig .10. Concentration profile for various Sc values when $Pr = 0.5, Nr = 10, n = 2, M = 2$

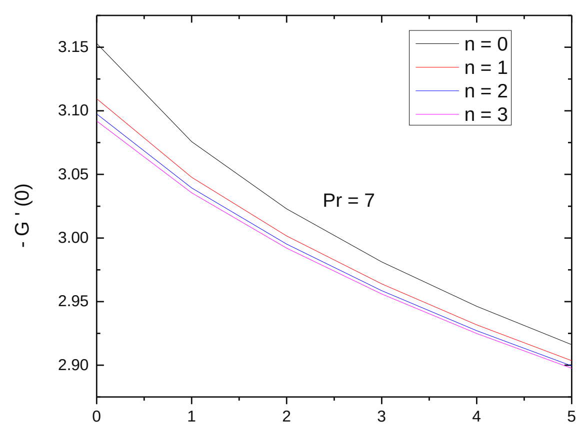

Fig .13.Variation of heat transfer rate with M and n when $Sc = 0.23, Nr = 10, s = 0.3$.

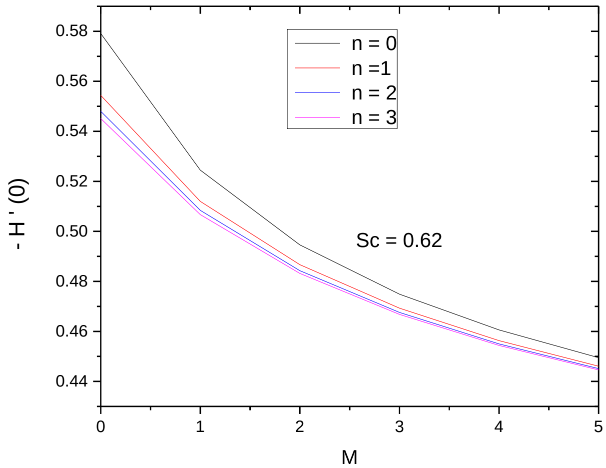

Fig .14. Variation of concentration with M and n when $Pr = 7, Nr = 10, s = 0.3$.

Table I. Skin friction coefficient, Surface heat transfer rate, and Surface mass transfer rate for some values of the parameters in the absence of magnetic field.

Pr	Sc	s	n	$-f''(0)$	$-G'(0)$	$-H'(0)$
0.7	0.23	0.0	0.0	0.6283	0.4609	0.2711
0.7	0.23	0.0	0.5	0.8901	0.4369	0.2616
0.7	0.23	0.0	1.0	1.0005	0.4273	0.2579
0.7	0.23	0.0	2.0	1.1014	0.4190	0.2579
0.7	0.23	-0.5	0.5	0.6636	0.2786	0.2111
0.7	0.23	0.0	0.5	0.8901	0.4369	0.2616
0.7	0.23	0.5	0.5	1.1823	0.6355	0.3210
0.7	0.23	1.0	0.5	1.5325	0.8679	0.3905
0.7	0.1	0.5	0.5	1.1823	0.6355	0.2280
0.7	0.62	0.5	0.5	1.1823	0.6355	0.6374
0.7	1.0	0.5	0.5	1.1823	0.6355	0.9385
0.7	2.0	0.5	0.5	1.1823	0.6355	1.6433
1.0	0.62	0.5	0.5	1.1823	0.8477	0.6374
5.0	0.62	0.5	0.5	1.1823	3.1240	0.6374
7.0	0.62	0.5	0.5	1.1823	4.1304	0.6374
10.0	0.62	0.5	0.5	1.1823	5.5856	0.6374

Table II. Skin friction coefficient $-f''(0)$, Surface heat transfer rate $-G'(0)$, and Surface mass transfer rate $-H'(0)$ for fixed values of some parameters in the presence of magnetic field $\Pr = 5.0, Sc = 0.62, s = 0.3, n = 0.5, Nr = 10.0$

M	$-f''(0)$	$-G'(0)$	$-H'(0)$
0.0	1.0578	2.4194	0.5531
0.2	1.1601	2.4032	0.5400
0.5	1.2975	2.3816	0.5237
1.0	1.4966	2.3508	0.5025
5.0	2.5596	2.1994	0.4270
10.0	3.4370	2.0940	0.3928

NOMENCLAUTURE

u, v	:	velocity components along x, y axis
υ	:	Kinematic velocity
ρ	:	Density of the fluid
σ	:	Electrical conductivity of the fluid
T	:	Nanofluid temperature
T_∞	:	Ambient temperature as $y \to \infty$
T_w	:	Temperature at stretching surface
C	:	Nanoparticle concentration
C_∞	:	Ambient concentration as $y \to \infty$
C_w	:	Concentration at stretching surface
C_f	:	Skin friction coefficient
Pr	:	Prandtl number
H	:	Dimentionless concemtration
Sc	:	Schmidt number
Sh_x	:	Local Sherwood number
s	:	Suction/injection parameter
Nr	:	Thermal Radiation parameter
n	:	Non-linear stretching parameter
q_r	:	Radiative heat flux
Cp	:	Specific heat at constant pressure
D	:	Mass diffusivity
U_w	:	Surface velocity
B_0	:	Induced magnetic field
M	:	Magnetic parameter

REFERENCES

[1] N.Afzal, A. Badaruddin, A.A.Elgarvi, *Int.J.Heat and Mass Transfer.* 36, 3399 (1999).
[2] R. Cortell, *Int.J.Nonlineaar Mech.*29, 155(1994).
[3] B.K.Dutta, P.Roy, *Int.Commun.Heat Mass.12, 89(1985).*
[4] L.G.Grubka, K.M.Bobba, *ASME J.* Heat Transfer.107, 248(1985).
[5] C.K .Chen, M.I.Char,.*J.Math.Anal.Appl.*,135, 568 (1988).
[6] V.Kumaran, A.V.Kumar, I.Pop, *Commun Nonlinear Sci Numer Simulat.*15, 300 (2010).
[7] N.Bakar, W.Zaimi, R.Hamid, B.Bidin, A.Ishak, *World Appl Sc J.*17, 49 (2012).
[8] F.M.Ali, R. Nazar, N.M.Arifin, I.Pop, *Appl.Math.Mech.Engl Ed*. 35, 155 (2014).
[9] K.Zaimi, A.Ishak, I.Pop, *Sci rep.*4, 404 (2014).
[10] R.Bhargava, LKumar, H.S.Takhar, *Int.J.Eng.Sci.*41,2161(2003)
[11] K.Battacharyya, *Ain Shams Engi.J.*4, 259(2013).
[12] M.Ferdows, S.M.Chappal, A.A.Afifty, *J.Engg.Thermophysiscs.*23, 216 (2014).
[13] N.A.Kelson, A.Desseaux, *Int.J.Eng.Sci.*39, 1881(2001).
[14] S.Mukopadhyaya, *Int.J.Heat Mass Transfer.*52,5213(2009)
[15] R.CoRtell, *Appl.Math.Comput.*184, 864(2007).
[16] K.V.Prasad, Kvajravelu, P.S.Datti, *Int.J.Nonlinear Mech.*45, 320(2010).
[17] P.Rana, R.Bhargava, *Comm.Nonlinear Sci Num Simul.*17,212(2012).
[18] W.Ibrahim and B.Shankar, *ASME. J. Heat Transfer.* 134, 112001(2012).
[19] Y.Yirga and B.Shankar, *J.Nanofluid.*2, 283 (2013).
[20] W.Ibrahim and B.Shankar, *J.Nanofluid.*4, 16(2015).
[21] R.CoRtell, *Appl.Math.Comput.*206, 832(2008).